International Journal of Engineering & Technology, 7 (4.14) (2018) 339-342

International Journal of Engineering & Technology

Website: www.sciencepubco.com/index.php/IJET

Research paper

Non-Acidic Method for Isolation of Microcrystalline Cellulose From Oil Palm Empty Fruit Bunch Fiber

N. Samat[1]*, N.N. Ghazali[1], Z. Ahmad[1], F. Ali[2]

[1]*Department of Manufacturing and Material Engineering Faculty of Engineering, International Islamic University Malaysia, Jalan Gombak 53100, Gombak, Kuala Lumpur, Malaysia*

[2]*Department of Biotechnology Engineering, Faculty of Engineering, International Islamic University Malaysia, Jalan Gombak 53100 Gombak Kuala Lumpur Selangor*

**Corresponding author E-mail: noorasikin@iium.edu.my*

Abstract

In this study, the microcrystalline cellulose (MCC) was extracted via a non-acidic method from the oil palm empty fruit bunch (EFB) cellulose. The extraction was conducted through Ammonium Persulfate (APS) oxidation treatment, which was followed by the ball milling process. The effects of varied temperature levels from APS oxidation treatment (60, 80 and 90^{o}C) and different milling time (1, 4 hours) were investigated. APS oxidation treatment at 90^{o}C was found to produce the most optimum results. The size of the MCC was less than 20µm and had demonstrated the highest degree of crystallinity index and thermal stability. The high crystallinity index is associated with the removal of non-cellulosic components as seen from FTIR analysis, where a decrease was observed in the characteristic peak intensity of 1735 and 1510 cm^{-1}. The milling time had also affected the formation of MCC. Although a relatively longer milling time had produced smaller MCC with narrow size distribution, it had, however, given rise to a slight adverse effect on the crystallinity index and thermal stability.

Keywords: *microcrystalline cellulose; oil palm empty fruit bunch; Ammonium Persulfate; ball mill; thermal*

1. Introduction

Malaysia is known as one of the world's largest palm oil producers. In 2017, there were 5.81 million hectares of oil palm plantations recorded, which indicates that there had been a 1.28% growth as compared to 2016 (1). However, the large plantation area had also generated a massive amount of oil palm biomass residue, where one of the palm oil industry wastes is the empty fruit bunches (EFB). Similar to other agricultural plants like cotton, kapok, bamboo, coconut and pineapple, the main constituents of EFB are cellulose, hemicellulose and lignin. While these cellulose exhibits outstanding mechanical properties such as a high Young's modulus associated to its crystalline structures, the hemicellulose and lignin, however, possess opposite structure and characteristics (2). For this reason, cellulose is favoured over its hemicellulose and lignin counterparts.

Microcrystalline cellulose (MCC) is a fine, white, odourless, crystalline powder and a biodegradable material that is used in a large range of applications such as in the pharmaceutical, food and paper industries (3). The increase in environmental consciousness and community interest had attracted researchers to use MCC as reinforcement in polymer composites (4-6). As such, the availability of large EFB fibres quantities has made it a suitable candidate as an alternative source for the MCC.

The MCC is obtained after the removal of its amorphous phases, where the common method used to produce or isolate the MCC is through acid hydrolysis (7). However, the use of highly concentrated acid seems to be the main drawback of this technique as the dilution and heating of the acid during the hydrolysis process would make it extremely corrosive. The difficulty of recycling used acid could also affect the environment considerably (8). This limitation can be addressed by using Ammonium Persulfate (APS); a strong oxidizing agent that is not only cheap but also exhibits low long-term toxicity with high water solubility (9). Furthermore, the acid hydrolysis method is also time-consuming and produces a low yield result (10). For these reasons, ball milling with the help of APS oxidation treatment had proven to be an interesting technique used in producing MCC due to its simple operation that generates large quantities of MCC. The aim of this research is to produce MCC from EFB fibre through the combined non-acidic method (APS oxidation treatment) and ball milling process. In this study, the influence from different (i) temperature levels used during APS oxidation treatment and (ii) milling hours was determined. The FTIR, XRD, TGA and morphological analysis were then carried out on the isolated MCC.

2.1 Materials

The oil palm empty fruit bunch (EFB) fibres obtained from the Malaysian Palm Oil Board (MPOB) were cut and passed through a 50 µm sieve, while the 98% Ammonium Persulfate (APS) was purchased from Bumi Pharma Sdn. Bhd.

2.2 APS treatment

7 g of EFB fibres were added into 1M APS solution, where the mixture was heated at different temperature levels (60^{o}C, 80^{o}C and 90^{o}C) using a hot plate and was subjected to 16 hours of constant stirring. The suspension was centrifuged at 10000 rpm for 10 minutes and then washed with distilled water to reach a pH level

close to 4. The samples were sonicated in an ice bath for 30 minutes and freeze-dried.

2.3 Ball Milling technique

1 g of EFB90 sample were ball milled using planetary pot mill (P-5, Fritsch) at a speed of 200 rpm. The ratio of tungsten carbide to cellulose was fixed at 60:1 and the ball milling process was carried out for 1 and 4 hours respectively. The treatment condition of the EFB fibres and its notation are listed in Table 1.

Table 1: Notation of sample

Sample	APS oxidation temperature (^{o}C)	Milling time (hour)
EFBRAW	-	-
EFB60	60	-
EFB80	80	-
EFB90	90	-
EFB90BM1	90	1
EFB90BM4	90	4

2.4 Characterization

The changes of the chemical bonding after undergoing the APS treatment were determined by using Fourier Transform Infrared Spectroscopy (FTIR) (Perkin Elmer FTIR), where the samples were scanned in the range of 380-4000 cm^{-1}.
The X-ray diffraction (XRD) patterns were obtained at 40 kV and 40 mA using an Ultima IV, Rigaku, X-ray diffractometer. A Cu K-α radiation was used and the spectrum was recorded from 10 to 50^{o} at a scan rate of 2 s/step with 0.02^{o} step size. The crystallinity index was calculated based on Eq. 1 (11):

$$C(\%) = \frac{Imax - Imin}{Imax} \times 100 \quad (1)$$

where,
I_{max} : maximum intensity of peak between 21^{o}-22.5^{o}
I_{min} : the amorphous peak intensity between an angle of about 18.6^{o} in the valley between the peaks
The thermal properties of all samples were investigated using thermogravimetric analyser (TGA) (STA 7300, Hitachi). The weight loss was determined starting from room temperature to 700^{o}C with a heating rate of 10^{o}C/min under an argon flow of 100 ml/min.
The sample was sputter coated with palladium before the morphology of cellulose was characterized through the use of scanning electron microscopy (SEM JSM 5600) at an acceleration voltage of 7.0 kV.

3. Result and discussion

3.1 FTIR analysis

The FTIR spectra of EFB fibre as well as the untreated and treated APS at 60, 80 and 90^{o}C are shown in Figure 1. Two prominent broad bands that are assigned to the characteristic of cellulose are seen in all samples, in which 3500-3200 cm^{-1} and 1051- 1025 cm^{-1} had corresponded to different O-H and C-O-C pyranose stretching modes respectively (5,12). The peak at 2900 cm^{-1} is attributed to C-H stretching whilst the small peak that appeared at 896 cm^{-1} had been due to celluloseic β-glycosidic linkages between the glucose units in cellulose (13-15).
The chemical reaction that had occurred during APS oxidation was evident from the changes shown in the FTIR spectra. A decrease in peak intensity was observed at peak 1735cm^{-1}, where it had corresponded to the C=O stretching of acetyl and uronic ester groups in hemicellulose or the ester linkage of the carboxylic groups in the p-coumaric units of the lignin (16). Another peak, which characterizes the lignin, is at 1510cm^{-1} and refers to C=C stretching as a result of the vibration in the aromatic lignin ring (17). According to (16) and (18), the decrease in peak intensity at both peaks indicates that most of the hemicelluloses and lignin had been extracted or removed during the oxidation process. The comparison of FTIR spectra in Figure 1 shows that the intensity of the decline in both peaks had been most prominent in sample EFB90. This implies that the amount of lignin and hemicellulose had been effectively reduced as compared to lower temperature levels (60 and 80^{o}C). The significant removal of both constituents had also resulted in the length and diameter reduction of the EFB fibre as demonstrated by the SEM micrographs.

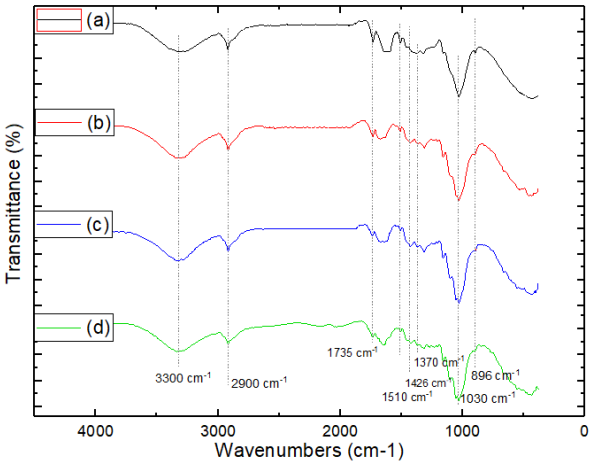

Fig. 1: FTIR spectra of a) EFBRAW b) EFB60 c) EFB80 d) EFB90

3.2 XRD Analysis

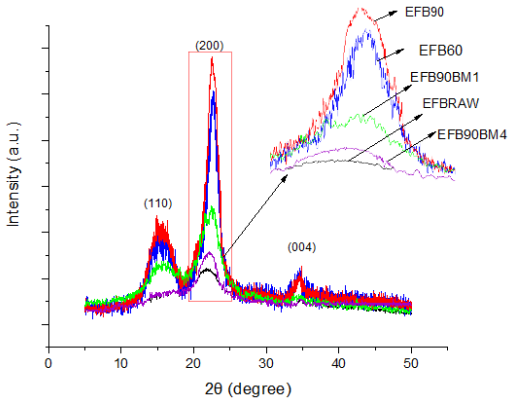

Fig. 2: XRD pattern of untreated EFB cellulose and treated cellulose through APS oxidation and ball milling under different conditions

The XRD studies were performed to analyse the crystalline behaviour of untreated, treated APS and ball milled EFB fibres. As depicted in Figure 2, the peaks at 2Θ = 15.5^{o}, 21^{o}, 22.5^{o} and 34.7^{o} had corresponded to the respective crystalline phase of (110), (200) and (004) of EFB cellulose (12, 19). All of the samples had exhibited a similar XRD diffractogram pattern, which implies that the crystal structure of cellulose in EFB fibres had remained unchanged even after undergoing the APS oxidation treatment and the ball milling process (13). However, the intensity of XRD spectrum had appeared to be different. This intensity reflects the crystallinity index (C). In this study, Eq. (1) was used to determine the C value and the result is tabulated in Table 2.
The APS treatment at 60^{o}C was found to have increased the crystallinity to about 25% as compared to EFBRAW. This can be attributed to the reduction or removal of the amorphous part through the breaking of glycoside linkage of the amorphous region during the APS treatment (20).

Table 2: Crystallinity of samples

Sample	Crystallinity index, C (%)
EFBRAW	43.10
EFB60	70.00
EFB90	75.24
EFB90BM1	60.98
EFB90BM4	60.31

The highest index value (C) obtained in sample EFB90 had been in accordance with the FTIR findings. The increase of the C value after APS oxidation had also been reported by (9), where they had used different source of cellulose such as flax, flax shives, hemp, MCC, wood pulp and bacterial cellulose. Moreover, the changes in the cellulose crystallinity had also been similar to the fibre being treated with acid degradation (15). Irrespective of milling time (Figure 2), the ball milling process had resulted in a decrease of the peak intensity in samples EFB90BM1 and EFB90BM4. This could be due to the strong shear effects of this process that had deteriorated the crystalline region of the cellulose (8).

3.3 TGA analysis

From Figure 3, all of the samples had exhibited three stages of thermal degradation. An initial weight loss that relates to the moisture evaporation in the fibre had occurred at an initial decomposition temperature of 15^{o}C and continued up to 125^{o}C with a mass loss of about 11% (16, 19). The decrease in the thermal stability as demonstrated by the second and third degradation stages of TGA spectra is associated with the decomposition of cellulosic materials (19).

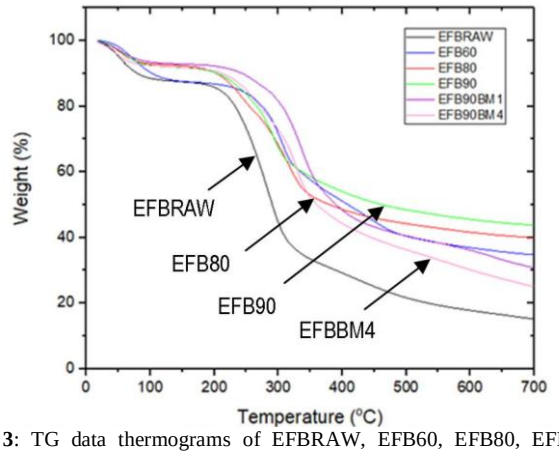

Fig. 3: TG data thermograms of EFBRAW, EFB60, EFB80, EFB90, EFB90BM1 and EFB90BM4

The following discussion touches on the degradation temperature range of 160 – 530^{o}C, which is related to the decomposition process that comes after the thermal degradation stages. The untreated or EFBRAW had shown the greatest weight loss of 68% in the respective temperature range. As for sample EFB60, although it had decomposed at a similar temperature range to that of EFBRAW (160^{o}C), its weight loss was only 49%. This result implies that there had been an increase in the thermal stability of EFB60, which was reflected by the higher crystallinity shown by the XRD analysis.

The decomposition temperature of samples EFB80, EFB90, EFB90BM1 and EFB90BM4 was observed to have shifted to a lower temperature level (140^{o}C) as compared to samples EFBRAW and EFB60. Their weight loss had also been lesser than that of EFBRAW (<60%). The decrease in the decomposition temperature of these samples suggests that higher temperature levels of APS treatment along with the ball milling process had turned the EFB fibres into smaller sizes or finer particles. Consequently, the large surface area of the fine particle would induce decomposition to occur at a lower temperature level (21). The weight loss experienced in the main degradation temperature range is summarized in Table 3.

The benefits of enhanced cellulose crystallinity on its flame resistance property are seen in Table 3. From the XRD result, the EFB90 that possessed the greatest crystallinity at 700^{o}C had shown the highest residual weight of 43%. Mandal and Chakrabarty (22) had also reported a finding that was similar to the current study. While the nanocellulose of sugarcane baggase was found to have a lower decomposition temperature (373^{o}C) as compared to the raw cellulose (385^{o}C), their residual weight, however, had been 15.58% and 7.68% respectively.

Table 3: Thermal properties of EFB samples

Samples	Thermal degradation range (^{o}C)	Weight loss in the respective degradation range (%)	Residual weight at 700 ^{o}C (%)
EFBRAW	160-530	68	15
EFB60	160-530	49	34
EFB80	140-530	48	39
EFB90	140-530	44	43
EFB90BM1	140-530	55	30
EFB90BM4	140-530	57	25

3.4 SEM

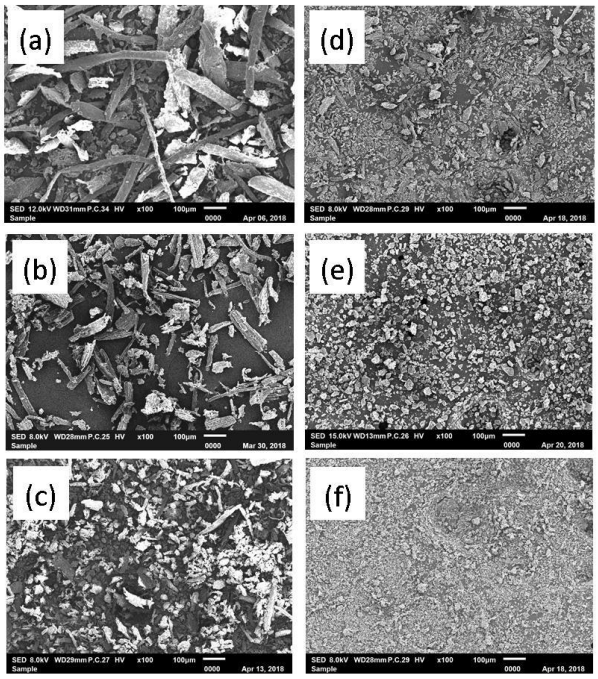

Fig. 4: SEM images of raw and treated samples under magnification of 100X. a) EFBRAW b) EFB60 c) EFB80 d) EFB90 e) EFB90BM1 f) EFB90BM4

Compared to the other samples, the untreated or EFBRAW (Figure 4a) had a larger dimension with a diameter and length of about 50µm and 300µm respectively. The EFB fibre dimension had appeared to decrease after the APS oxidation treatment (Figure 4b-d), where the influence of temperature on the fibre size reduction had been a more pronounced at higher temperature levels. When the temperature level was raised from 60 to 90^{o}C, it was observed that the fibre diameter had decreased by about twofold (from 34.75 µm to 15.94 µm). The length of the fibrils had also been greatly reduced along with the increased temperature levels. The high temperature levels had therefore resulted in an increased concentration of free radicals generated from APS chemical, which led to a strong oxidation reaction (13). As a result, a larger amorphous region could be extracted from the EFB fibres.

In Figure 4e, it is evident that the ball milling process had assisted in the further reduction of the small EFB fibre into fine cellulose (6.74 µm). The longer milling time (4 hours) had also produced finer cellulose of about 3.31 µm (Figure 4f) with a narrow particle size distribution. Hence, it is presumed that the extension of milling hour would raise the occurrence of ball-to-cellulose collision. This phenomenon may possibly increase the breakup of hydrogen bonding between the cellulose and led to the formation of smaller cellulose (11).

4. Conclusion

The microcrystalline cellulose (MCC) was successfully obtained by using a non-acidic method (APS oxidation) and the ball milling process. The FTIR analysis had demonstrated the extraction of hemicellulose and lignin during the APS oxidation to be more significant at a higher temperature level (90^{o}C). This observation was in full agreement with the XRD results, where the respective sample was shown to exhibit the highest crystallinity index of 75%. The high crystallinity index of MCC had also enhanced its thermal stability. From the SEM micrographs, it was revealed that the APS oxidation treatment had reduced the length and diameter of the EFB fibre. The ball milling process at a longer milling time had also assisted in the production of smaller size cellulose. While a longer milling time had reduced the size of MCC efficiently, it had, however, resulted in the deterioration of the crystalline region.

Acknowledgement

The authors thank the International Islamic University Malaysia (IIUM) for the support of this research.

References

[1] Malaysia Palm Oil Council (MPOC) (2017), "Annual Report", available online: http://mpoc.org.my/default.aspx

[2] Ejikeme PM (2008), Investigation of the physicochemical properties of microcrystalline cellulose from agricultural wastes I: Orange mesocarp. *Cellulose* 15, 141–147.

[3] Li X, Tabil LG & Panigrahi SC (2007), Chemical treatments of natural fibre for use in natural fibre-reinforced composites: A review. *Journal of Polymer Environment* 15, 25–33.

[4] Lazim NH & Samat N (2017), The influence of irradiated recycled polypropylene compatibilizer on the impact fracture behavior of recycled Polypropylene /Microcrystalline cellulose composites. *Polymer Composites*, doi.org/10.1002/pc.24430.

[5] Zulkifli NI, Samat N, Anuar H & Zainuddin N (2015), Mechanical properties and failure modes of recycled polypropylene/microcrystalline cellulose composites, *Materials and Design* 69, 114–123.

[6] Kiziltas A, Gardner DJ, Han Y & Yang HS (2011), Thermal properties of microcrystalline cellulose-filled PET–PTT blend polymer composites, *Journal of Thermal Analysis and Calorimetry* 103, 163-170.

[7] Ashori A & Nourbakhsh A (2010), Performance properties of microcrystalline cellulose as a reinforcing agent in wood plastic composites. *Composites Part B* 41, 578–81.

[8] Luo X & Wang X (2017), Preparation and characterization of nanocellulose fibers from naoh / urea pretreatment of oil palm fibers. *BioResources* 12(3), 5826–5837.

[9] Leung ACW, Hrapovic S, Lam E, Liu Y, Male KB, Khaled AM & Luong JHT (2011), Characteristics and Properties of Carboxylated Cellulose Nanocrystals Prepared from a Novel One-Step Procedure. *Small* 7(3), 302-305.

[10] Tang LR, Huang B, Ou W, Chen XR & Chen YD (2011), Manufacture of cellulose nanocrystals by cation exchange resin-catalyzed hydrolysis of cellulose, *Bioresource Technology* 102, 10973-10977.

[11] Zhang L, Tsuzuku T & Wang X (2015), Preparation of cellulose nanofiber from softwood pulp by ball milling. *Cellulose* 22(3), 1729-1741.

[12] Rayung M, Nor AI, Norhazlin Z, Wan ZS, Nur, IAR & Chieng BW (2014), The effect of fiber bleaching treatment on the properties of poly(lactic acid)/ oil palm empty fruit bunch fiber composites. *International Journal of Molecular Sciences*15(8) 14728-14742.

[13] Cheng M, Qin Z, Liu Y, Qin Y, Li T, Chen L, & Zhu M (2014), Efficient extraction of carboxylated spherical cellulose nanocrystal with narrow distribution through hydrolysis of lyocell fibers using ammonium persulfate as an oxidant, *Journal of Materials Chemistry A* 2, 251-258.

[14] Nasution H, Yurnaliza, Veronicha, Irmadani, & Sitompul (2017), Preparation and characterization of cellulose microcrystalline (mcc) from fiber of empty fruit bunch palm oil. *IOP Conf. Series: Materials Science and Engineering*, 180(1).

[15] Fahma F, Iwamoto S, Hori N, Iwata T & Takemura A (2010), Isolation , preparation , and characterization of nanofibers from oil palm empty-fruit-bunch (OPEFB). *Cellulose* 17(5), 977–985.

[16] Goh KY, Ching YC, Chuah CH, Luqman CA & Liou NS (2016), Individualization of microfibrillated celluloses from oil palm empty fruit bunch : comparative studies between acid hydrolysis and ammonium persulfate oxidation. *Cellulose* 23(1), 379–390.

[17] Chen W, Yu H, Liu Y, Chen P, Zhang M & Hai Y (2011), Individualization of cellulose nanofibers from wood using high-intensity ultrasonication combined with chemical pretreatments. *Carbohydrate Polymers*, 83(4), 1804-1811.

[18] Ferrer A, Alciaturi C, Faneite A & Ríos J (2016), Analyses of Biomass Fibers by XRD, FT-IR and NIR. In Silvio, V. J. (Ed.). Analytical Techniques and Methods for Biomass *Springer-Verlag* ,Switerland, pp. 45-83.

[19] Phanthong P, Guan G, Ma Y, Hao X, & Abudula A (2016), Effect of ball milling on the production of nanocellulose using mild acid hydrolysis method. *Journal of the Taiwan Institute of Chemical Engineers* 60, 617-622.

[20] Md Ziaul K, Zaira ZC, Sharifah, BAH & Md Eaqub A (2014). Statistical optimization for acid hydrolysis of microcrystaline cellulose and its physiochemical characterization by using metal ion catalyst. *Materials* 7, 6982-6999.

[21] Sofla MRK, Brown RJ, Tsuzuki T & Rainey TJ (2016), A comparison of cellulose nanocrystal and cellulose nanofibres extracted from baggase using acid and ball milling methods. *IOP Conf. Series: Advances in Natural Sciences: Nanoscience and Nanotechnology* 7.

[22] Mandal A & Chakrabarty D (2011), Isolation of nanocellulose from waste sugarcane bagasse (SCB) and its characterization. *Carbohydrate Polymers* 86(3), 1291-1299.